10.21611/qirt.2016.045

The development of contact and noncontact technique to study the heat dissipation in metals under loading

by A. Iziumova*, A. Vshivkov* and O. Plekhov*

* ICMM UB RAS, 1 Ac. Koroleva Str., 614013 Perm, Russia, fedorova@icmm.ru

Abstract

This work is devoted to the development of experimental technique allowing the analysis of energy balance in metal specimens during mechanical test and construction of heat sources field. The use of infrared thermography (IRT) is connected primarily with problem of definition of the time constant related to the heat losses. The goal of this work is to develop the technique which allows avoiding the additional experiments consisting in cooling test to find heat losses constant. Proposed technique is a combination of contact (heat flux sensor) and noncontact (IR camera) equipment which could be used during mechanical test.

1. Introduction

Nowadays infrared thermography (IRT) is widely used in different areas of life such as medicine [1], defectoscopy [2], warfare, security control etc. Also IRT has an important application in scientific researches as a relatively simple noncontact method of temperature measurement of object surface. There are a lot of works devoted to study of material state under deformation on the basis of so-called energy approach, where IRT is used to determine the mechanical [3, 4] and thermal characteristics [5, 6, 7] and to evaluate the damage degree of material by construction of heat source field of material surface. According to the last task determination of time constant related to heat losses plays an important role in accuracy of such calculations and in assessment of energy balance of materials under loading conditions. Usually the additional cooling test is performed to define this constant.

In present work the heat flux sensor is proposed to avoid additional experiment and to find the required time constant during mechanical test directly. This sensor consists of two Peltier elements. One of them plays a role of heat stabilizer. Another one is used for measurement of potential drop U (in Volts) which appears because of the temperature difference between plates of Peltier element (Peltier–Seebeck effect).

The main goal of this work was to compare standard method of determination of time constant related to heat losses and proposed technique based on heat flux sensor in real conditions of mechanical test.

2. Materials and experimental conditions

In this work titanium alloy specimens (Ti-0.8Al-0.8Mn) were tested under quasistatic tensile conditions. Smooth dog-bone-shaped specimens (figure 1) were used.

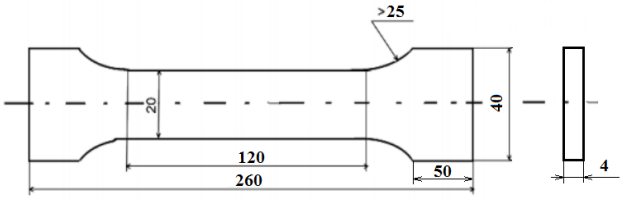

Fig. 1: *Geometry of specimen for tensile testing*

Specimens surface on the one side were specially prepared for infrared record before testing. Preparation consisted of two stages. In the first step specimen's surface was polished by abrasive paper with different grain sizes. The second step was to coating the polished surface by a thin layer of amorphous carbon to decrease the emissivity of surface. Another side of specimens was used for installation of the heat flux sensor. To provide a good thermal contact the specimen surface under heat flux sensor was coated by thermal paste.

Figure 2 shows the scheme of the experimental setup consisting of electric mechanical testing machine Shimadzu AG-X Plus (300 kN), IR camera FLIR SC5000, heat flux sensor and video extensometer Shimadzu TRViewX240S. The characteristics of the IR camera are the followings: a spectral range of 3–5 μm, a maximum frame size of 320 × 256 pixels, a spatial resolution of 10^{-4}m and a temperature sensitivity of 25 mK at 300 K. The calibration of the IR camera was made on the basis of the standard calibration table. To exclude an influence of internal sources on the experimental conditions, experimental setup was covered by black screen. IR camera and heat flux sensor record data continuously during mechanical test.

Figure 3 illustrates a true stress-strain curve obtained experimentally. The strain rate was $15 \cdot 10^{-4}$ sec^{-1}.

10.21611/qirt.2016.045

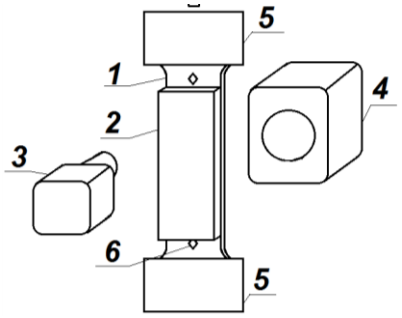

Fig. 2: *Scheme of experimental setup (1 – specimen, 2 – heat flux sensor, 3 – video extensometer, 4 – infrared camera, 5 – grips of the testing machine, 6 – reference points for video extensometer)*

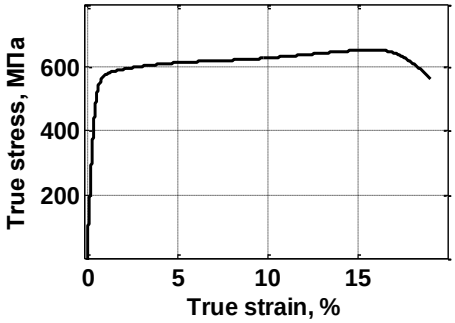

Fig. 3: *True stress-strain curve for titanium alloy Ti-0.8Al-0.8Mn*

The developed heat flux sensor is described in details in [8]. This sensor consists of two Peltier elements. One of them plays a role of heat stabilizer. Another one is used for measurement of potential drop U (in Volts) which appears because of the temperature difference between plates of Peltier element. Calibration function (1) shows the dependence between heat flux in Watts and potential drop in Volts.

$$W = 0,006U + 0,0042\,. \tag{1}$$

Heat flux sensor allows us measuring the heat flux on the specimen surface during mechanical test in combination with IR camera. As a result of experiment the stress-strain curve of titanium alloy Ti-0.8Al-0.8Mn, evolution of temperature field of specimen surface and heat flux were obtained by video extensometer, IR camera and heat flux sensor, respectively.

3. Determination of time constant

From mechanical point of view in such experiments the main goal of infrared data processing is to calculate a heat source field during quasistatic test and to evaluate the energy balance in materials under deformation before damage. As a result this information is used in energy based approach to propose a criterion of damage.

Usually to calculate a heat source field caused by plastic deformation, heat conductivity equation (2) is applied to infrared thermography data.

$$\rho c \frac{\partial T(\mathrm{x,y,z,t})}{\partial t} = Q(\mathrm{x,y,z,t}) + k\left(\frac{\partial^2 T(\mathrm{x,y,z,t})}{\partial x^2} + \frac{\partial^2 T(\mathrm{x,y,z,t})}{\partial y^2} + \frac{\partial^2 T(\mathrm{x,y,z,t})}{\partial z^2} \right), \tag{2}$$

where $T(x,y,z,t)$ – temperature field, ρ – material density (4475 kg/m3), c – heat capacity (569 J/(kg·K)), k – heat conductivity (14 W/(m·K)), $Q(x,y,z,t)$ – heat sources field, x,y,z – coordinates, t – time. Thermal constants of investigated titanium alloy were specified by authors on the base of technique described in details in [9]. In general this technique is modification of standard flash method [10]. The main feature of it is possibility to define the heat conductivity and heat diffusivity simultaneously during the same experiment.

Infrared camera allows one to register the temperature field on the specimen surface without control of temperature distribution in thickness of specimen. This is the reason of using enough thin specimens in experimental investigations. It makes possible to assume that the temperature distribution in thickness is homogeneous. Heat conductivity equation in such case has to be averaged on z-coordinate (thickness). The standard operation of averaging [11] was used. Difference $\theta'(x,y,t)$ between average temperature and temperature of environment was written as follows:

$$\theta'(x,y,t) = \frac{1}{h}\int_{-h/2}^{h/2} (T(\mathrm{x,y,z,t}) - \mathrm{T_0})\,dz = \theta(\mathrm{x,y,t}) - \mathrm{T_0}, \tag{3}$$

where T_0 – initial temperature of environment in thermal equilibrium, h – specimen thickness.

Boundary conditions expressed as:

$$\left.\frac{\partial \mathrm{T}(x,y,\mathrm{z},t)}{\partial \mathrm{z}}\right|_{z=\frac{h}{2}} = -\left.\frac{\partial \mathrm{T}(x,y,\mathrm{z},t)}{\partial \mathrm{z}}\right|_{z=-\frac{h}{2}}$$
$$-\mathrm{k}\left.\frac{\partial \mathrm{T}(x,y,\mathrm{z},t)}{\partial \mathrm{z}}\right|_{z=\frac{h}{2}} = \frac{\beta 1}{h}\int_{-h/2}^{h/2}(T(\mathrm{x},\mathrm{y},\mathrm{z},\mathrm{t})-\mathrm{T}_0)\,dz, \quad (4)$$

where *β1* – heat exchange coefficient in perpendicular direction to specimen surface.

Considering expressions (3) and boundary conditions (4), integration of equation (2) allows one to obtain relation (5) for determination of heat source field caused by plastic deformation during specimen testing.

$$Q_{\mathrm{int}}(x,y,t) = \rho c\left(\dot{\theta}(x,y,t) + \frac{\theta(x,y,t)-\mathrm{T}_0}{\tau}\right) - k\Delta\theta(x,y,t), \quad (5)$$

where $\theta(x,y,t)$ is temperature field on specimen surface, $\Delta\theta(x,y,t)$ is Laplace operator of temperature field, $Q_{int}(x,y,t)$ is heat source field (W/m^3), τ is time constant which is related to the heat losses [11, 12].

As a result numerical finite difference scheme of equation (5) applying to the IR data could allow us to calculate the heat source field using infrared data.

Figure 4 illustrates the area of interest for calculation of heat source field to compare infrared camera data and data of heat flux sensor with a goal of time constant τ assessment. Such choice of area is due to the size of heat flux sensor. During deformation the specimen is extended. Heat flux sensor is fixed on a special rigid support and just put to the specimen. It means as if the specimen slides under the sensor. Despite of that a good thermal contact provided by thermal paste between the specimen and sensor allows registering the heat flux at all stages of deformation.

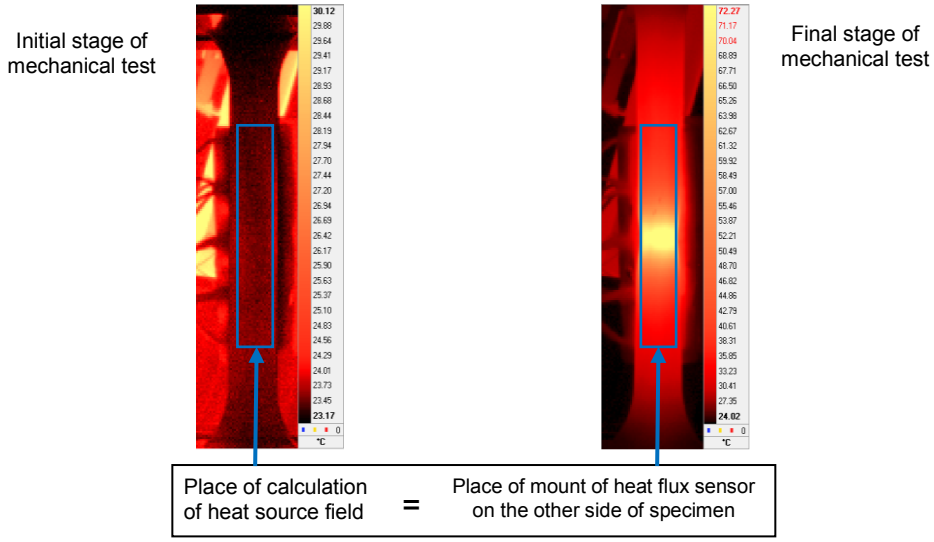

Fig. 4: *Place of heat sources field calculation to assess time constant τ*

In this work the time constant τ was evaluated by two ways. The first one was the standard method of cooling test after local point heating of specimen surface [13]. The second way was using the data of heat flux sensor and infrared camera.

3.1. Standard procedure of time constant determination (cooling test)

Before beginning of mechanical test, temperature measurements of the specimen surface after point heating were performed. In this work the heterogeneous heating was provided by momentary contact with the soldering-iron.

To evaluate time constant τ the heat conductivity equation (5) with zero heat source value was used:

$$0 = \dot{\theta}(x,y,t) + \frac{\theta(x,y,t)-\mathrm{T}_0}{\tau} - \alpha\Delta\theta(x,y,t), \quad (6)$$

where α is thermal diffusuvity.

To obtain correct results, the experimental temperature data was filtered both in time and in space using standard Gaussian kernel. Results of filtering procedure are presented in figure 5 and 6. Figure 5 illustrates field of temperature change after momentary local heating. Cuts 1 and 2 marked in figure 5 are shown in figure 6A and B. Figure 6C presents original data (solid line) and time filtered data (dashed line) in the point with maximum temperature marked in figure 5 by symbol "O". Data processed by filter demonstrate satisfactory correlation with original data.

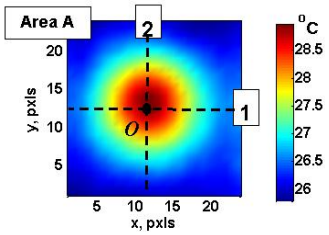

Fig. 5: *Temperature field after momentary local heating*

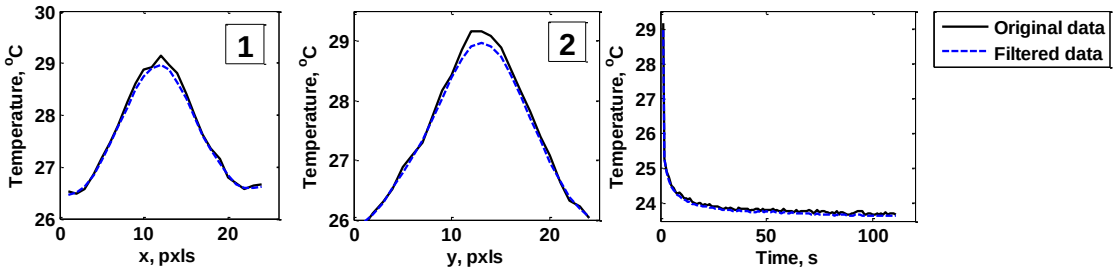

Fig. 6: *Illustration of data filtering: A and B – original data (solid line) and space filtered data (dashed line) along the section 1 and 2, respectively, C – original data (solid line) and space filtered data (dashed line) in the point with maximum temperature*

The time derivation and the Laplace operator of temperature field in equation (6) were calculated separately by using the method of forward finite difference scheme realized in Matlab. Then each term in equation (6) was integrated over the square area "A" limiting the hot spot marked in figure 5.

To define time constant τ the criteria (7) was used.

$$\sum\left(\dot{\theta}_A(t)+\frac{\theta_A(t)}{\tau}-\alpha\left(\Delta\theta\right)_A(t)\right)^2\rightarrow 0, \tag{7}$$

where subscript "A" means integration over the area A.

Figure 7A and B show the time dependence of each term in expression (6) and their sum with the optimal value of the time constant τ according to the criteria (7).

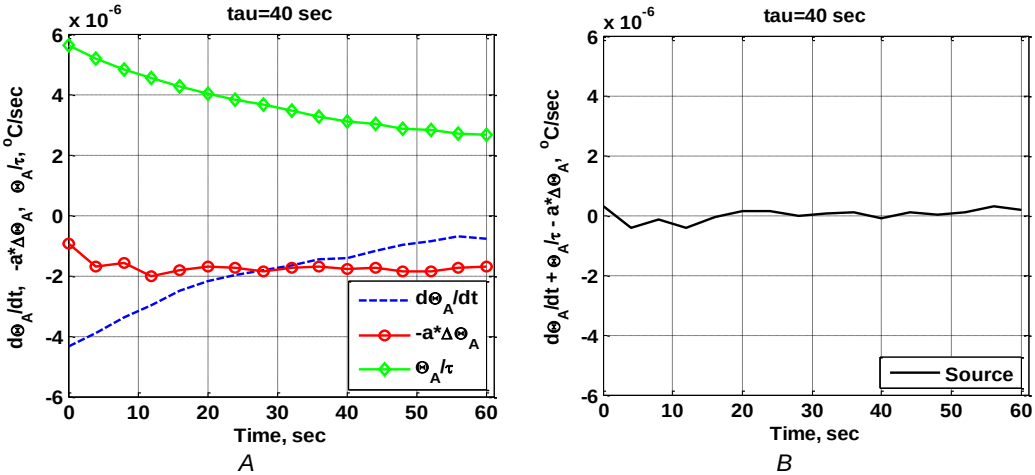

Fig. 7: *A – time dependence of terms of the expression (6), B – sum of terms in equation (6) versus time with τ determined by criteria (7).*

As it is shown in Figure 7B the sum of terms in expression (6) which is equal to heat source value, is close to zero. This result was obtained with optimal value of time constant of 40 s.

3.2. Applying of heat flux sensor to time constant definition

Heat flux sensor directly registers heat flux under self-surface in time during mechanical test. To compare this data with heat calculated by IR data, heat source field obtained by equation (5) was integrated in length and width of interest area (figure 4):

$$Q_{IR}(t) = e\int_0^a\int_0^b Q_{\text{int}}(x,y,t)dxdy, \tag{8}$$

where *a* and *b* – corresponding length and width of interest area, *e* – thikness of specimen.

The time constant *τ* was picked out so as to provide a good correlation between heat sources values obtained by contact sensor and on the basis of IRT data. The heat flux versus time obtained by contact sensor and on the basis of infrared thermography data with *τ*=42 s is presented in figure 8.

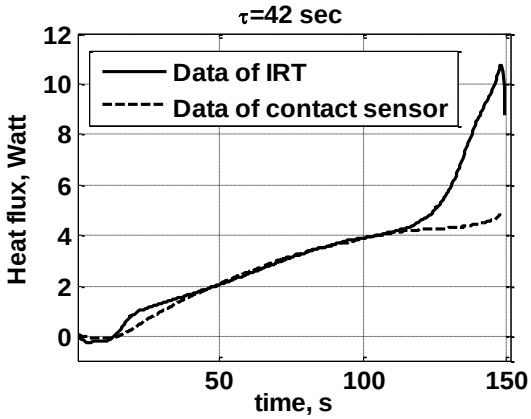

Fig. 8. *Illustration of time constant determination by data of heat flux sensor and IRT data*

Data in figure 8 demonstrate a good agreement from 40 to 110 seconds. Significant differences in data after 110 sec could be explained by starting of large plastic deformation and changing of material density and heat capacity. That is why in the last stage of deformation (after 15 %) the calculation of heat flux by heat conductivity equation (5) is not correct. Figure 9 illustrates heat flux versus deformation before 15% of strain.

Data obtained by IRT and using contact sensor are in a good agreement from 4 to 15% of strain when heat flux was changed gradually. In figure 10 red color show limit of applicability of proposed technique on stress-strain curve. Poor correlation of data at the beginning part of experiment could be explained by thermal inertia of heat flux sensor to the fast changes of heat sources.

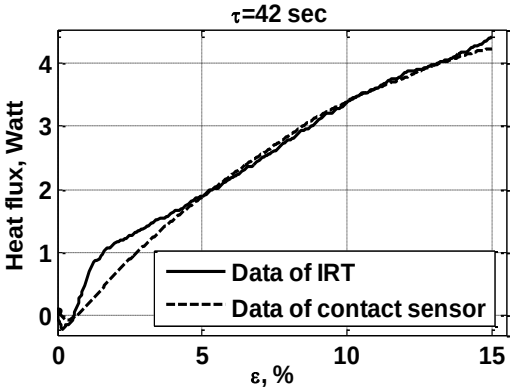

Fig. 9: *Heat flux obtained by IR data (τ =42 s) and contact sensor versus strain*

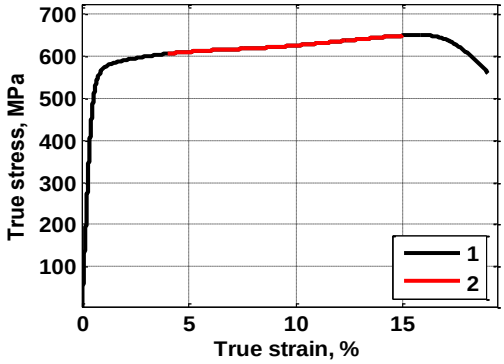

Fig. 10: *1 – stress-strain curve of titanium alloy Ti-0.8Al-0.8Mn; 2 – limits of applicability of proposed technique on stress-strain curve*

The time constant related to the heat losses which is calculated on area coating of sensor (area of interest in figure 4), is valid for full specimen in current conditions. That is why when we have defined time constant, heat source field could be determined on any part of specimen surface, and energy balance could be constructed for full specimen.

4. Conclusions

As a result the time constant τ was determined by standard procedure of cooling test after point heating of the specimen surface and using developed technique based on applying of heat flux sensor. In the first case value of time constant was 40 seconds, in the second case this constant was 42 seconds. Proposed technique requires some improvements to increase the accuracy of time constant determination and to overcome the inertia effect of contact sensor. Despite of that preliminary results allow us to conclude that proposed technique of measurement the time constant could be used in experimental works. Data of time constant related to the heat losses which were obtained by two ways demonstrated satisfactory agreement. Developed technique allows to avoid additional experiments of cooling after point heating and to find the required time constant during mechanical test directly. So that, proposed technique reduces time of experiment and provides enough precise result of time constant τ.

ACKNOWLEDGMENTS

The reported study was funded by RFBR according to the research project No.16-31-00130 мол_а and No.14-01-00122.

REFERENCES

[1] Lahiri B.B., et al., Medical applications of infrared thermography: A review, Composites Science and Technology. – Vol. 69, pp. 1131–1141, 2009.
[2] Vavilov V.P., Świderski W., Derusova D., Ultrasonic and optical stimulation in IR thermographic NDT of impact damage in carbon composites, Quantitative InfraRed Thermography Journal. – Vol. 12, Is. 2, pp. 162-172, 2015.
[3] La Rosa G., Risitano A., Thermographic methodology for rapid determination of the fatigue limit of materials and mechanical components, International Journal of Fatigue. – Vol. 22, pp. 65-73, 2000.
[4] Punnosen S., Mukhopadhyay A., et al., Determination of critical strain for rapid crack growth during tensile deformation in aluminide coated near-α titanium alloy using infrared thermography, Materials Science & Engineering. –Vol. A 576, pp. 217-221, 2013.
[5] Dong H., Zheng B., Chen F., Infrared sequence transformation technique for in situ measurement of thermal diffusivity and monitoring of thermal diffusion, Infrared Physics & Technology. – Vol. 73, pp. 130-140, 2015.
[6] Martínez K., et al., Thermal diffusivity measurements in solids by photothermal infrared radiometry: Influence of convectioneradiation heat losses, International Journal of Thermal Sciences. – Vol. 98, pp. 202-207, 2015.
[7] Massard H., Fudym O., Orlande H.R.B., Batsale J.C., Nodal predictive error model and Bayesian approach for thermal diffusivity and heat source mapping, C. R. Mecanique. – Vol. 338, pp. 434–449, 2010.
[8] Vshivkov A., Iziumova A., Plekhov O., Bär J., Experimental study of heat dissipation at the crack tip during fatigue crack propagation, Fracture and Structural Integrity. – Vol. 35, pp. 131-137, 2016.
[9] Zhelnin M., Iziumova A. and Plekhov O., The determining thermal constant of metals by infrared thermography, AIP Conference Proceedings (In press).
[10] Tseng-Wen Lian et all., Rapid thermal conductivity measurement of porius thermal insulation material by laser flash method, Advanced Powder Technology. – Vol. 1, pp. 1-4, 2016.
[11] Boulanger T., Chrysochoos A., Mabru C., Galtier A., Calorimetric analysis of dissipative and thermoplastic effects associated with the fatigue behavior of steel., International journal of fatigue. – Vol.26, pp. 221-229, 2004
[12] Chrysochoos A., Louche H., An infrared image processing to analyse the calorific effects accompanying strain localization, International journal of engineering science. – Vol. 38, pp. 1759-1788, 2000.
[13] Chrysochoos, A., Balandraud, X. and Wattrisse, B., Identification procedure using full-field measurements applications in mechanics and structures, Proc. of CNRS summer school, Montpellier, 2-5, 2013.